Impedance measurement methods for assessing the performance of Fuel Cells and Li-ion batteries in on-board applications

Jules MILLET[1], Daniel DEPERNET[1], Ali SARI[2], Frédéric GUSTIN[3], Hugo HELBLING[2]
[1]Université Marie et Louis Pasteur, UTBM, CNRS, Institut FEMTO-ST, FCLAB, F-90000 Belfort, France
[2]Université Claude Bernard Lyon 1, Ampère, UMR5005, INSA Lyon, Ecole Centrale de Lyon, CNRS, Villeurbanne, F-69100, France
[3]Université Marie et Louis Pasteur, CNRS, Institut FEMTO-ST, FCLAB, F-90000 Belfort, France

E-Mail : jules.millet@utbm.fr / daniel.depernet@utbm.fr / ali.sari@univ-lyon1.fr / frederic.gustin@univ-fcomte.fr / hugo.helbling@univ-lyon1.fr

ACKNOWLEDGMENT

This work has been supported by the EIPHI Graduate school (contract "ANR-17-EURE-0002" and the Region of Bourgogne Franche-Comté).

The HYSySPEM project was funded by the "France 2030" government investment plan managed by the French National Research Agency, under the reference ANR-22-PEHY-0018.

The work was done thanks to the 'Decentralized energy production' project, directed by EFFICACITY, the French R&D Institute for urban energy transition.

***Index Terms*—EIS, Battery, Fuel cell, Impedance measurement, Signal processing, Harmonic injection.**

***Abstract*—This study focuses on the characterization of fuel cells and batteries to assess their State of Health (SoH) using electrochemical impedance spectroscopy (EIS) in an on-board setting. The characterization methods include both active and passive EIS techniques, complemented by robust signal processing algorithms. Initial simulation results demonstrate the potential of impedance analysis for accurate SoH estimation. In addition, the implementation on a Texas Instruments board highlights the practical challenges associated with real-time programming, paving the way for future optimization and deployment in real-world applications.**

I. INTRODUCTION

At the heart of the energy transition, the mobility sector remains one of the main sources of carbon dioxide (CO_2) emissions [1]. In recent years, efforts have been made to replace internal combustion engines with electric motors. The latter run on electrical energy supplied by batteries or fuel cells, significantly reducing CO_2 emissions during use. As part of the France 2030 investment plan, research programs have been launched to develop these technologies. The HYSySPEM project, which includes this work, aims to optimize these systems for heavy-duty vehicles, such as trucks and ships.

Hydrogen electric vehicles are currently classified as hybrid vehicles, relying on multiple energy sources: a fuel cell to meet the energy demand during low dynamics and a battery to manage the transition phases. The aging of these power sources is a central focus of current research. However, before reaching the end of their lifespan, it is essential to determine how these power sources will be characterized in an on-board context. One proposed solution is the use of electrochemical impedance spectroscopy (EIS).

II. ON-BOARD IMPEDANCE MEASUREMENT

EIS is based on the application of a sinusoidal excitation signal through the source, at a given frequency and to a fixed operating point, in order to analyze the voltage and current response [2]. By repeating this process over a wide range of frequencies, it becomes possible to determine the impedance spectrum. However, in the case of on-board use, where no laboratory equipment is available, it is necessary to find a method of generating an excitation signal. One solution is proposed by D. Depernet et al. [2], who suggest performing signal injection via the converter by modulating the duty cycle. However, given the architecture imposed in the HYSySPEM project, converters are not always present at the source level, which means that several methods of EIS could be used to obtain the impedance of each system (Fig. 1).

In the case of a fuel cell, fitted with a converter, the signal injection must be as non-disruptive as possible and last for the shortest time possible. In the literature, this type of EIS is referred to as active EIS. However, in the case of a battery without a converter, where direct injection of excitation signals is not possible, an alternative method must be explored. Several articles mention the concept of passive EIS [2]–[4], which involves analyzing the frequency content of battery voltage and current signals in dynamic operation. Dynamic operation refers to acceleration or deceleration phases generated by the vehicle user. This is why the precision of the driving cycle is crucial to the study. It is therefore essential to define the correct energy management for the chosen power architecture.

As shown in the article by S. Luciani et al. [5], in this type of case, the fuel cell is used to generate slightly variable currents, while the battery compensates for transients. In our case study, this choice of energy management is perfectly suited to correctly characterize the two electrochemical sources using the EIS methods proposed in the literature. In addition to presenting these different methods, the aim is to propose a robust signal processing algorithm that can exploit both methods.

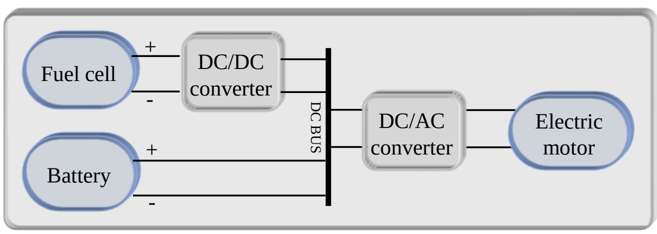

Fig. 1. Power architecture HYSySPEM project

A. Active EIS applied fuel cell

Active EIS involves applying a low-amplitude sinusoidal current at different frequencies to a fixed operating point. More precisely, it means injecting an alternating current superimposed on a slightly variable direct current (Fig. 2).

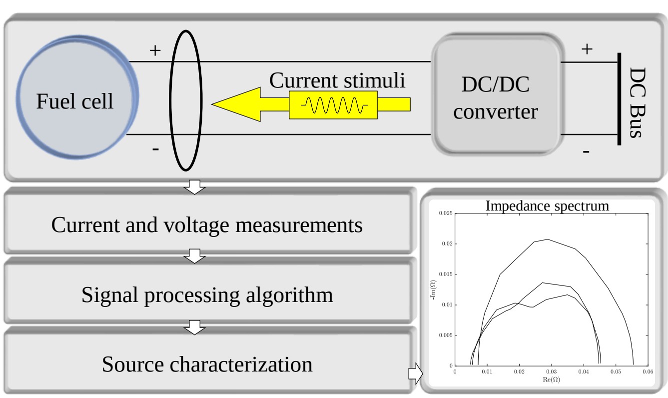

Fig. 2. Active EIS application

In the on-board context, perfect steady-state operation is rare, so what is traditionally done is to block the source using the power converter [2]. The complication with this method is that, because the source is blocked at a fixed operating point, the battery has to manage the power flow on its own, which can be challenging in some cases. The injection of the current stimuli must therefore be as efficient as possible, i.e., sweep the frequency range as quickly as possible. This is because, if the current, temperature, or health of the fuel cell varies, so does the impedance, and the impedance measurement becomes inaccurate. Non-sinusoidal injection signals can therefore be used to optimize this time. Several studies and articles explore this approach, laying the foundations for early research in this field. E. Sadeghi et al. explore a large number of possible signals for this type of application, such as triangle, square-wave, multi-sine, PRBS, and white noise excitations, and conclude that multi-sine and PRBS are the most promising [6].

M. Zhang et al. propose other types of signals, one in particular being highly coherent with the desired approach: the chirp signal, which automatically scans the entire frequency range [7]. A similar approach to the one mentioned above is proposed by M. Koseoglou et al. [8], which involves continuously injecting a chirp-type signal and analyzing the response obtained for each frequency as it is applied. In a publication by N. Lohmann et al. [9], three types of signals are compared: rectangular, Gaussian, and cardinal sine (sinc). From this study, the sinc and Gaussian signals appear to be the most promising and efficient for this type of application.

The optimization of measurement time to reduce signal injection is a well-developed subject, enabling impedance to be calculated just as accurately at the injected frequency.

B. Passive EIS applied battery

Passive EIS aims to evaluate system impedance without using excitation signals. The current and voltage signals must therefore be analyzed for frequency disturbances. These disturbances can be induced by acceleration, deceleration, the driving environment, or even other power converters (Fig. 4). Lohmann et al. [10] present similar work, analyzing the frequency content of a driving cycle. The Goertzel algorithm is used, which assumes that the frequencies of interest are already known. This study lays the foundation but presents a case where the signal processing algorithm searches exclusively for injected frequencies, as if the battery were a white box. B. Liebhart et al. address part of this subject and seek to obtain the impedance of a lithium-ion battery in a dynamic regime (driving cycle) without injecting signals [11]. By applying a robust signal processing method, they succeed in calculating the system impedance, providing a solid basis for further research. More recently, B. Yang et al. [4] reused part of the OPEIS method, previously presented by Liebhart et al. [11], and applied it to different driving cycles in urban, mountainous, and rural environments. The results are promising, as they treat the battery data like a black box, i.e., without prior knowledge of the frequency content. This study also highlights the limitations of OPEIS acquisition and application.

In light of the various avenues explored in recent years, the study of the driving cycle appears to be a viable approach for obtaining battery impedance. However, this type of analysis is not straightforward, as the impedance of a battery, like that of a fuel cell, varies significantly not only with current but also with temperature [10], [12]. This underscores the need for a robust signal processing method capable of accurately calculating impedance.

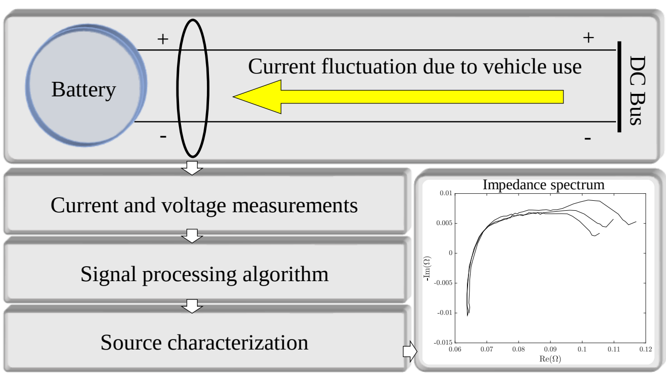

Fig. 4. Passive EIS application

III. Signals processing method

Whether discussing active or passive EIS, a signal processing algorithm must be implemented to calculate impedance in the dynamic regime.

In the literature, two methods are presented for analyzing this type of signal: one calculates the impedance directly from the voltage and current signals [9], while the other calculates it from the power spectral density [3]. The goal is to build upon existing work to develop a reliable and robust method. The decision was made to focus on using raw current and voltage signals, as this method is considered reliable for characterization. The next step is to optimize this approach to obtain accurate impedance measurements in both passive and active EIS (Fig. 3). Furthermore, to ensure the highest possible precision, a series of methods will be implemented to validate the calculated measurements.

A. *Signals segmentation*

Signal segmentation is one of the most crucial aspects of the method. This approach, previously proposed by several researchers [3], [4], [13], involves dividing the received signals, V(t) and I(t) (voltage and current), into numerous small segments. The segments are then categorized into three different frequency ranges (TABLE I): LF (Low-Frequency), MF (Medium-Frequency), and HF (High-Frequency). The frequency ranges are selected based on the electrochemical properties of the power sources. Batteries will have a broader frequency range due to more significant inductive phenomena [14].

TABLE I
Fuel cell & battery frequency ranges

Frequency ranges	Fuel cell	Battery
LF	0.1 to 10 Hz	0.1 to 25 Hz
MF	10 to 100 Hz	25 to 250 Hz
HF	100 to 1000 Hz	250 to 3000 Hz

The purpose of this approach is to optimize data acquisition, enabling accurate detection of all the fre-

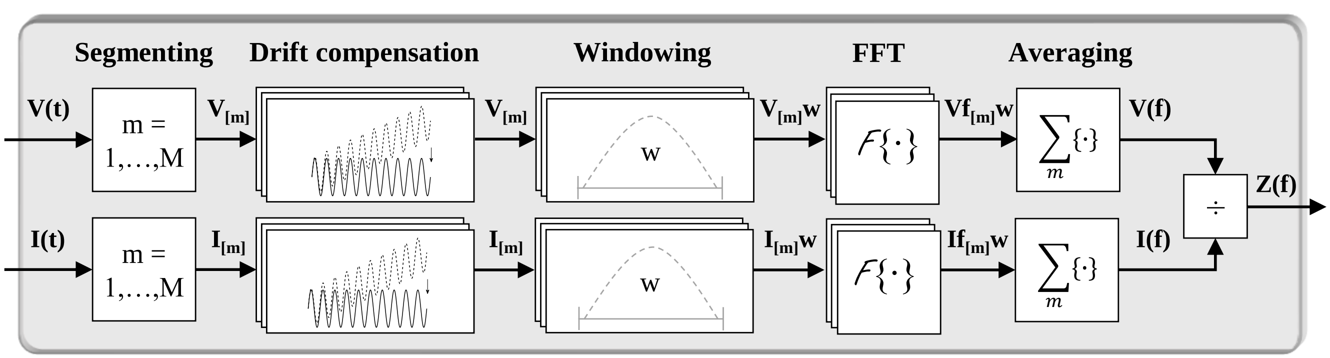

Fig. 3. An optimized method for impedance spectroscopy

quencies present. Several other important parameters can be used to further refine the results (Fig. 5).

- N = Number of points per segment
- R = Overlap rate
- M = Total number of segments
- L = Signal length

The number of points per segment depends on the number of periods to be considered for the Discrete Fourier Transform (DFT) and the number of points per period. The overlap rate decreases with the frequency range to maintain approximately constant calculation dynamics of the frequency components. Once the V(t) and I(t) signals have been segmented, the segments go through a validation stage.

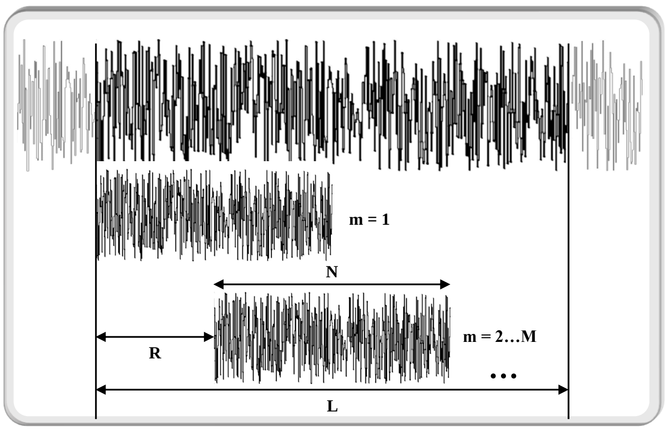

Fig. 5. Division of data into M overlapping segments of length for low-frequency

B. Drift compensation

This is a key step in the performance of this algorithm. Indeed, to correctly apply the Discrete Fourier Transform (DFT), certain conditions must be met [15]. The system must be causal (response only due to the applied perturbation), linear (follows linear differential laws), stationary (time-invariant and at steady state), and stable (maintains consistent behavior over time). For the purpose of analyzing driving cycle frequencies, these conditions are not always met. This is why methods are available to address some of these issues [15]:

- Real time drift compensation
- Time course interpolation

Not all methods can be applied before the DFT, as some operate directly on time-domain signals, while others work on frequency-domain signals. Therefore, initially, only drift compensation will be implemented. This method helps eliminate disturbances caused by non-linearity (Fig. 6). In practice, this compensation is achieved using filters, as presented by D. Depernet et al. [2]. However, there is currently no method for compensating for the system's lack of stability, which remains a significant issue that can distort the overall reliability of the measurement.

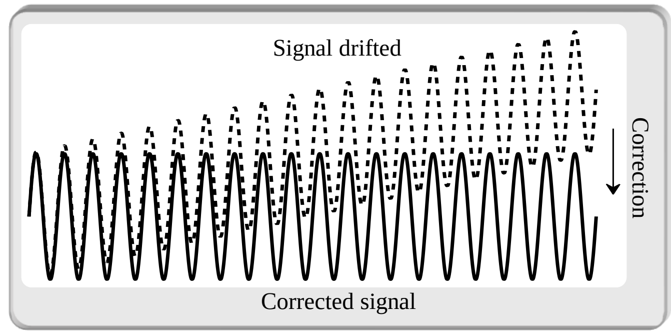

Fig. 6. The real-time drift compensation of the sinusoidal perturbation

That's why we chose to eliminate segments with poor stability, i.e., segments with high impedance variation. In the low-frequency range, there is a higher likelihood of impedance variation due to the longer segment duration (Fig. 7).

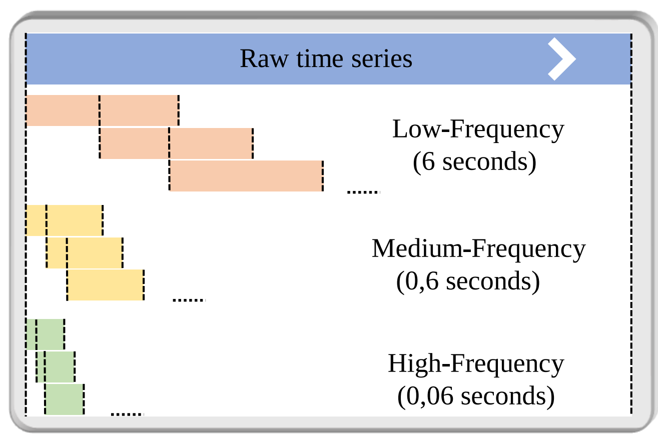

Fig. 7. Segments variation time

C. Windows & DFT

Before applying the DFT, a windowing operation must be performed, as the signals under study are non-periodic [13]. More specifically, frequencies can distort the spectrum obtained, a phenomenon known as spectral leakage. However, a DFT is applicable to periodic signals, so to mitigate some of the undesirable effects associated with the study of non-periodic signals, windowing is performed. The choice of window is therefore of prime importance in mitigating spectral leakage.

In articles presenting the spectral analysis of driving cycles, Gaussian windows [9], Hamming windows [3], and Hanning windows [4] are used instead of rectangular windows.

Once the signals have been segmented, validated, and windowed, the DFT can be applied. This allows us to move from the time domain to the frequency domain. Widely used in the literature [2], [12], this method is reliable. However, the question arises of whether to use the FFT (Fast Fourier Transform) algorithm to reduce computation times (TABLE II).

TABLE II
COMPARISON DFT AND FFT METHODS

Criteria	**DFT**	**FFT**
Definition	The DFT is a transformation that converts a finite sequence of values into a sequence of frequency coefficients.	The FFT is an optimized algorithm to compute the DFT more quickly.
Time complexity	$O(N^2)$	$O(N*\log(N))$
Conditions of use	No specific conditions, can be used for any N	Typically requires N to be a power of 2 for classical FFT algorithms
Example (N=1024)	$1024^2 = 1048576$ operations	$1024*\log^2(1024)$ =10240 operations

The FFT is an optimized version of the DFT and is much faster due to its reduced computational complexity, making it essential for processing large signals. There are two possible approaches, depending on the electronic board to be used.

D. Impedance Calculation, Averaging, and Validation

After applying the DFT with a Hamming window, the impedance is calculated at the detected frequencies [2], [12]. A validation method, briefly presented in the 'Drift Compensation' section, is necessary to verify the measurement. This validation involves the Impedance High-precision Identification Technique (Z-HIT), used, for instance, in Zahner software, which is based on Kramers-Kronig [16] and Hilbert relations [15]. These relations allow for the calculation of the real and imaginary parts of a complex function from one another, thereby estimating the error between the measured and calculated curves, ensuring linearity and stability [3]. Finally, impedance averaging is performed over a certain number of segments, determined by the frequency range and system stability. A segment that detects a frequency at a specific operating point cannot be averaged with a segment that detects the same frequency two minutes later or under different operating conditions.

IV. PARTICAL APPLICATIONS

Now that the method has been implemented, it must be tested through simulation based on experimental data using Matlab/Simulink. For this purpose, a fuel cell model based on transfer functions was developed, with its parameters determined through experimental measurements. In addition, a converter was modeled to best replicate real operating conditions, allowing for the injection of excitation signals. To validate the algorithm, the method is first applied to the modeling of the fuel cell. Then, the method is tested on the battery test bench with real measurements.

A. Method Validation on an Experimental Fuel Cell Model

To test the algorithm under optimal conditions, experimental data are used. Impedance spectra were obtained at different current levels on the fuel cell under well-defined experimental conditions (Fig. 8).

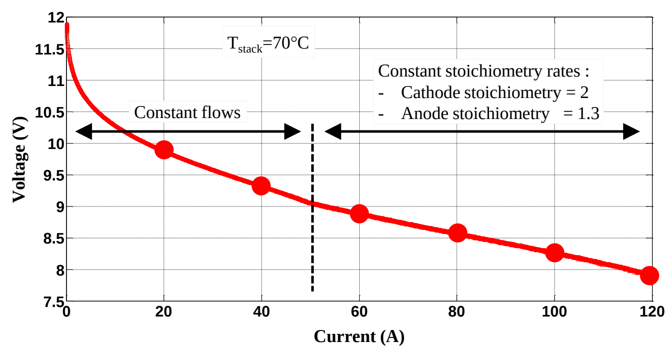

Fig. 8. Polarization curve and operating point where the EIS measurements were performed

Using an optimization algorithm [17] and an equivalent electrical model (Fig. 9), it is possible to determine the model parameters, without any faults, as a function of the current.

These parameters are then used in a model that represents the characterized electrochemical behavior of the fuel cell. For example, in Fig. 9, the variation of the resistor 'Rm' as a function of the current is shown.

Thereafter, we used this model to extrapolate the operation of the PEMFC under dynamic current conditions. This model is subsequently reused to test various aspects of the signal processing method. The benefit of examining the proper functioning of the method on the fuel cell lies in the ability to know the injected frequencies, allowing for comparison with the reference.

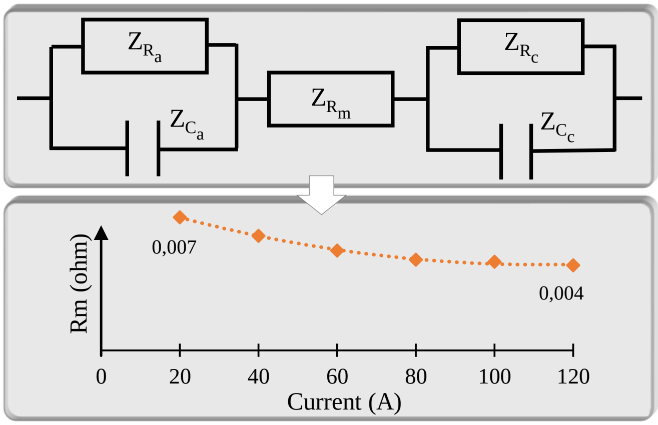

Fig. 9. Fuel cell equivalent electrical model representation and Parameter Rm as a function of the current

The first test involves injecting several sinusoidal signals at a fixed operating point (40A) within the previously presented frequency ranges. The goal is to demonstrate that the algorithm works in a typical EIS case. Frequencies of 270 Hz, 60 Hz, 45 Hz, 18 Hz, 7.2 Hz, 3 Hz, and 0.6 Hz are injected. The spectrum shown in the graph below (Fig. 10) illustrates the evolution of impedance for each injected frequency over a duration of 15 seconds.

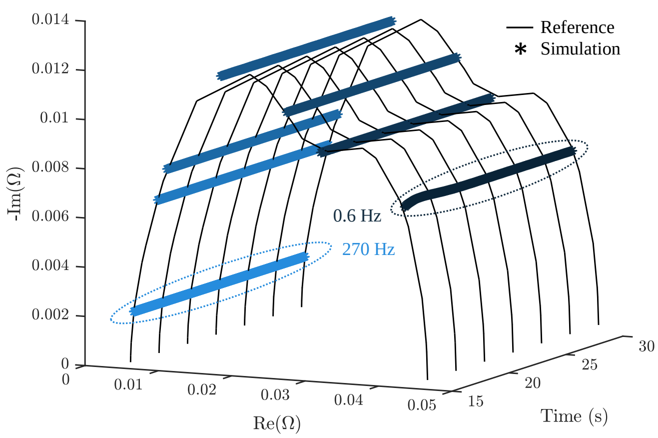

Fig. 10. Impedance spectrum versus time at a fixed operating point 40A

It is clear that there is no variation in impedance over time, as the measurement was conducted at a fixed operating point. The black curve represents the reference impedance spectrum at 40A, displayed every 3 seconds, while individual frequencies are highlighted in blue. For example, on the right side of Fig. 10, the evolution of the impedance at 0.6 Hz with respect to the current (dotted outline) can be observed.

Next, to simulate real operating conditions, a significant drift was introduced to determine whether the correct real impedance could still be identified.

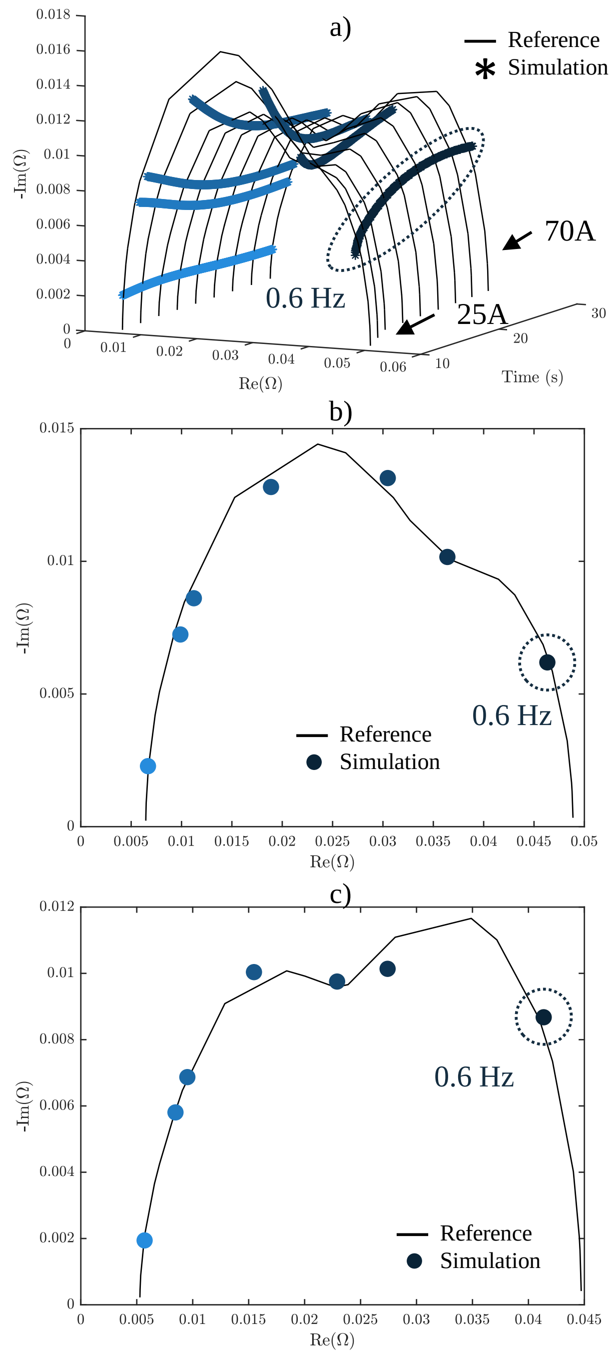

Fig. 11. a) Impedance variation between two operating points - b) Impedance spectrum averaged at 40A - c) Impedance spectrum averaged at 60A

Specifically, a linear current ranging from 25 A to 70 A was applied over a duration of 20 seconds, along with a multi-sinusoidal signal comprising high, medium, and low frequencies (the same frequencies as at the fixed operating point). This implies that the system is nonlinear and not in a steady state due to the drift and varying impedance. The signal processing algorithm was therefore applied to obtain impedance spectra under these conditions.

The impedance spectrum in Fig. 11 - a) below represents the overall result of the processing. Unlike the spectrum presented in the previous section, here the impedance varies, requiring the determination of multiple spectra for different operating points. It is evident that the impedance for each detected frequency changes with the current variation. To differentiate the various impedance spectra, the average operating point was calculated for each segment. Compared to the impedance spectra used, spectra were plotted at operating points of 40 A and 60 A (reference), and these spectra were compared to the simulation results. In Fig. 11 - b) and c), the segments corresponding to these operating points were selected and then averaged. The average is calculated over all the segments around the operating point, which varies over a period of 5 seconds. The results indicate that this method is effective, demonstrating that the algorithm can determine impedance spectra even when the system is nonlinear and unstable. Future tests will involve different types of drifts beyond a simple slope. However, initially, active EIS tests on the fuel cell can be performed under good conditions. Having tested with the measurements provided by the simulation, the next objective is to use real measurements.

B. Method Validation on Test Bench for Batteries

After validating the proper functioning of the signal processing algorithm on a fuel cell model, the next step is to evaluate its performance using real voltage and current measurements. For this purpose, an experimental bench dedicated to battery cell characterization is employed. This bench includes an electronic load capable of generating current stimuli and random signals. Using this setup, impedance measurements (EIS) can be performed.

On the test bench, an experimental scenario is defined for the first time (Fig. 12): applying a constant current (using current stimuli) to validate the quality of the measurements and the effectiveness of the signal processing algorithm. The frequency range varies between 1 Hz and 1000 Hz.

This scenario is designed to last only a few seconds to avoid significant variations in the state of charge (SoC), which strongly influence impedance values. The evaluation of these two scenarios will enable the validation of the algorithm using real experimental data. To

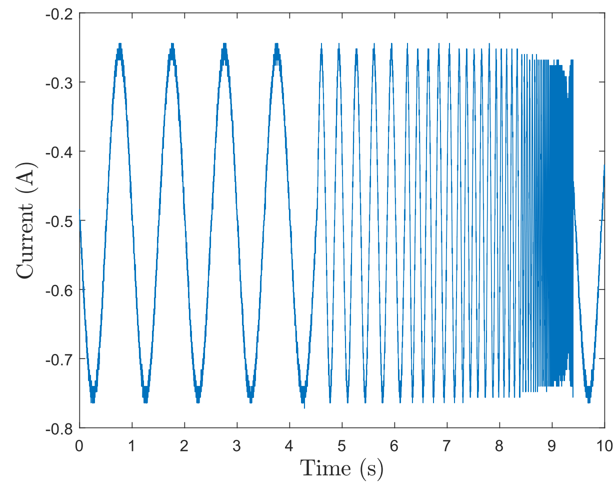

Fig. 12. Constant current discharge (0.5A) + Harmonic injection

validate the measurements, a highly accurate reference EIS is performed just before this scenario, allowing for a comparison of the measurements. This reference EIS is processed using a conventional signal processing algorithm, which operates by knowing the injected frequency and defining several parameters to ensure qualitative measurements (sampling frequency, number of points, number of periods, etc.). In contrast to the reference EIS, the scenarios are processed using the signal processing algorithm developed in this article. The figure below presents the impedance spectrum of both the reference and the scenario.

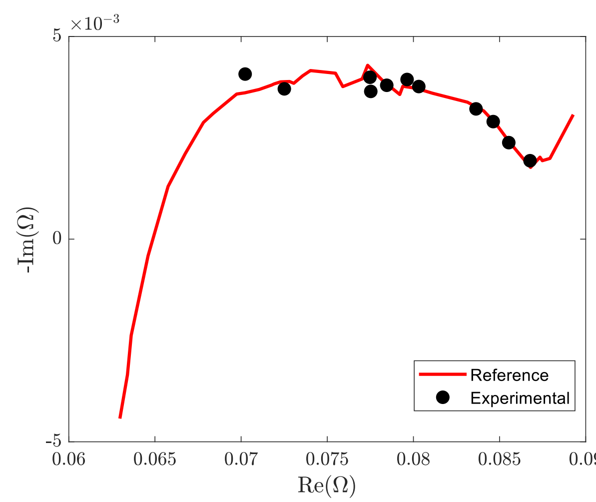

Fig. 13. Impedance spectrum processed with the new signal processing algorithm

By observing the experimental spectrum (Fig. 13), it is clear that it does not cover the entire frequency range. Indeed, the reference spectrum is performed over a frequency range from 3000 Hz to 0.1 Hz, whereas the scenario covers a range from 1000 Hz to 1 Hz. However, the impedance measurements remain consistent with the reference, further validating the algorithm.

In the future, the goal will be to test driving cycles. For now, however, the focus is on defining an implementation strategy for the electronic board.

C. Implementation

Now that a large part of the method has been tested in Matlab/Simulink and experimentally, it's time to move on to the implementation phase. The main objectives are to meet the processing time requirements for each segment and to manage the memory constraints of the board. It's crucial to ensure that the data arrays are correctly populated while making sure that the FFT and windowing operations are performed. For instance, with a 75% overlap, this means that four segments, and thus five arrays, operate in parallel. Each segment is shifted by 25% relative to the total number of points in the segment (Fig. 14).

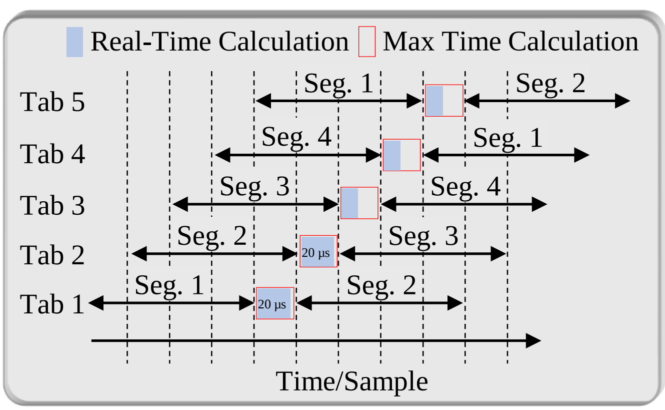

Fig. 14. Data segmentation with overlap and consideration of high-frequency computing time

This results in a time of 0.25 times the segment duration, depending on the frequency range. The most critical case arises at high frequencies, where the segments are shortest. In the high-frequency range, based on the simulations conducted, the duration of a segment is 50 ms, which is significantly shorter than what is required for the calculations. Specifically, a Texas Instruments TMS320F28379D microprocessor operating at 200 MHz is used. According to its documentation, for segments with 128 points, the windowing step takes 666 processor cycles, while the FFT calculation requires 3003 cycles (1).

$$T_c = \frac{N_{\text{windowing}} + N_{\text{FFT}}}{F_{\text{CPU}}} \approx 20\,\mu s \ll 0.25 \cdot 50\,ms \quad (1)$$

So, it is clear that the time taken to process each table (segment) before it can be reused is more than sufficient. The previous diagram illustrates the process with a 75% overlap rate (Fig. 14). The arrays are first populated, used for calculations, and then overwritten to make room for new data. This process will enable real-time calculation of impedance spectra.

V. Conclusion

This study highlighted a signal processing method, aimed in particular at characterizing a battery and a fuel cell using active and passive EIS techniques. Active EIS, which has been extensively utilized, facilitated the optimization of a signal processing algorithm for passive EIS. This research established the foundation for this algorithm and tested it in simulation and in experimental, demonstrating its effective performance. Although the algorithm has shown promising results for active EIS with the fuel cell, it still needs to be fully deployed in real driving cycles to identify its frequency characteristics.

Subsequently, the algorithm was tested on a battery test bench, enabling the analysis of real measurements. Whether applied to the simulation of the fuel cell or the battery test bench, spectra consistent with the references were obtained.

Future work will therefore focus on testing more complex signals to further validate the method. This advancement will subsequently enable real-time characterization of the battery and fuel cell, aiming to assess their health status.

References

[1] Forum International des Transports. *Perspectives des transports FIT 2023*. Perspectives des transports FIT. OECD.

[2] Daniel Depernet, Abdellah Narjiss, Frédéric Gustin, Daniel Hissel, and Marie-Cécile Péra. Integration of electrochemical impedance spectroscopy functionality in proton exchange membrane fuel cell power converter. 41(11):5378–5388.

[3] Bernhard Liebhart, Lidiya Komsiyska, and Christian Endisch. Passive impedance spectroscopy for monitoring lithium-ion battery cells during vehicle operation. 449:227297.

[4] Bowen Yang, Dafang Wang, Beike Yu, Facheng Wang, Shiqin Chen, Xu Sun, and Haosong Dong. Research on online passive electrochemical impedance spectroscopy and its outlook in battery management. 363:123046.

[5] Sara Luciani and Andrea Tonoli. Control strategy assessment for improving PEM fuel cell system efficiency in fuel cell hybrid vehicles. 15(6):2004.

[6] Erfan Sadeghi, Mohammad Mahdi Gholami, Mohsen Hamzeh, Seyed Mohammad Mahdi Alavi, and Mehrdad Saif. A systematic overview of power electronics interfaced electrochemical impedance spectroscopy for energy storage systems. 62:106850.

[7] Ming Zhang, Yanshuo Liu, Dezhi Li, Xiaoli Cui, Licheng Wang, Liwei Li, and Kai Wang. Electrochemical impedance spectroscopy: A new chapter in the fast and accurate estimation of the state of health for lithium-ion batteries. 16(4):1599.

[8] Markos Koseoglou, Evangelos Tsioumas, Dimitra Ferentinou, Nikolaos Jabbour, Dimitrios Papagiannis, and Christos Mademlis. Lithium plating detection using dynamic electrochemical impedance spectroscopy in lithium-ion batteries. 512:230508.

[9] Nils Lohmann, Patrick Weßkamp, Peter Haußmann, Joachim Melbert, and Thomas Musch. Electrochemical impedance spectroscopy for lithium-ion cells: Test equipment and procedures for aging and fast characterization in time and frequency domain. 273:613–623.

[10] Nils Lohmann, Peter Haussmann, Patrick Wesskamp, Joachim Melbert, and Thomas Musch. Employing real automotive driving data for electrochemical impedance spectroscopy on lithium-ion cells. 4(2):308–317.

[11] Bernhard Liebhart, Simon Diehl, Dominik Schneider, Christian Endisch, and Ralph Kennel. Enhancing the cell impedance estimation of a lithium-ion battery system with embedded power path switches. In *2021 IEEE Applied Power Electronics Conference and Exposition (APEC)*, pages 967–974. IEEE.

[12] Sudnya Vaidya, Daniel Depernet, Salah Laghrouche, and Daniela Chrenko. State of temperature detection of li-ion batteries by intelligent gray box model. 585:233624.

[13] Jérôme Antoni and Johan Schoukens. A comprehensive study of the bias and variance of frequency-response-function measurements: Optimal window selection and overlapping strategies. 43(10):1723–1736.

[14] François Paul Savoye. Impact des impulsions périodiques de courant sur la performance et la durée de vie des accumulateurs lithium-ion et conséquences de leur mise en oeuvre dans une application transport.

[15] C. A. Schiller, F. Richter, E. Gülzow, and N. Wagner. Validation and evaluation of electrochemical impedance spectra of systems with states that change with time. 3(3):374–378.

[16] M. Schönleber, D. Klotz, and E. Ivers-Tiffée. A method for improving the robustness of linear kramers-kronig validity tests. 131:20–27.

[17] Tummala.S.L.V. Ayyarao, Nishanth Polumahanthi, and Baseem Khan. An accurate parameter estimation of PEM fuel cell using war strategy optimization. 290:130235.